ELSEVIER

Polymer 41 (2000) 4869–4879

polymer

Optically active polyamides containing 1,3-dioxolane cycles in the backbone

J.I. Iribarren, A. Martínez de Ilarduya, C. Alemán, J.M. Oraison, A. Rodríguez-Galán, S. Muñoz-Guerra*

Departamento d'Enginyeria Química, ETSEIB, Universitat Politècnica de Catalunya, Diagonal 647, 08028 Barcelona, Spain

Received 25 May 1999; received in revised form 20 August 1999; accepted 29 September 1999

Abstract

The structure in the solid state of two optically active polyamides obtained from 2,3-*O*-methylene-L-tartaric acid and linear α,ω-alkanediamines with 9 and 12 carbon atoms, abbreviated P9MLT and P12MLT respectively, was investigated. Two ordered phases, one of smectic liquid crystal-type and another showing crystalline order, were characterized for P12MLT. Crystallization of the former into the second was induced by annealing. Infrared spectroscopy showed that hydrogen bonds are intermolecularly set in both phases and that they are weaker in the crystal phase. Quantum mechanical calculations found the O–C–C=O sequence of the tartaric unit to be in a *gauche* conformation. CP-MAS ^{13}C NMR revealed that the dioxolane ring is a mixture of the C_2-*exo* and C_2-*endo* puckered forms in equal amounts and that the polymethylene segment crystallizes in the all-*trans* conformation. X-ray diffraction of fibers and electron microscopy of solution grown single crystals afforded data consistent with a crystal lattice with orthorhombic geometry and parameters $a = 7.8$ Å, $b = 5.8$ Å, $c = 20.0$ Å. Experimental data obtained from P9MLT indicated a similar behavior for this system.

Keywords: Optically active polyamides; Poly(tartaramide)s; Carbohydrate-based polyamides

1. Introduction

Whereas a formidable amount of research on the crystal structure of conventional nylons [1–4] has been performed, the knowledge available on optically active non-polypeptidic polyamides is very limited. Most of the structural studies carried out on these systems are concerned with their conformation in solution [5] and only a few cases dealing with their structure in the solid state have been reported [6–10]. This is an unpleasant situation since optically active polyamides are promising materials where chiroptical effects can be combined with good mechanical and thermal properties.

Over the past several years, our group has devoted sustained efforts to investigate the synthesis, structure and properties of polyamides derived from carbohydrates [11,12]. Specific attention has been paid to poly(tartaramide)s, which are the polyamides made from naturally occurring tartaric acid (2,3-dihydroxy-succinic acid). Several classes of poly(tartaramide)s differing either in the group used for masking the hydroxyl side groups of the diacid unit [13,14] or in the diamine used as comonomer [15–17] have been examined. We found that poly(alkylene-di-*O*-methyl-L-tartaramide)s, i.e. polyamides made from 1,*n*-alkanediamines and 2,3-di-*O*-methyl-L-tartaric acid, crystallize in a triclinic lattice with slightly contracted chains arranged in hydrogen bonded layers which are stacked following a model close to that found in the α-form of nylon 6,6 [18]. Similar structures were also described for poly(tartaramide)s entirely derived from tartaric acid containing four stereocenters in the repeating unit [17]. In contrast with these results, helical structures stabilized by intramolecular hydrogen bonds have been proposed recently for certain glucose deriving polyamides on the basis of conformational data provided by NMR in solution [19,20].

This paper is concerned with the structure in the solid state of two optically active polyamides, namely poly(nonamethylene 2,3-*O*-methylene-L-tartaramide) and poly(dodecamethylene 2,3-*O*-methylene-L-tartaramide). They will be called here P9MLT and P12MLT, respectively, for consistency with nomenclature used in previously published work for other related poly(tartaramide)s [13].

* Corresponding author.
E-mail address: munoz@eq.upc.es (S. Muñoz-Guerra).

0032-3861/00/$ - see front matter
PII: S0032-3861(99)00716-8

Table 1
Data of polyamides examined in this work (data taken from Ref. [13])

Polyamide	$[\eta]$ (dl g^{-1})[a]	M_v[b]	M_w[c]	M_w/M_n[c]	$[\alpha]_D$ (deg)[d]	T_m (°C)[e]
P9MLT	0.60–0.80	8000–18,000	–	–	−12.2	90
P12MLT	0.90–1.30	22,700–47,200	24,500–44,100	2.4–1.6	−9.6	130

[a] Intrinsic viscosity measured in dichloroacetic acid at 25°C.
[b] Molecular weights calculated by applying the viscosimetric equation reported for nylon 6,6 [21].
[c] Molecular weights estimated by GPC of trifluoroacetylated samples.
[d] Specific optical rotation measured in chloroform ($c = 1$ g dl^{-1}; 25°C).
[e] Melting peak observed by DSC.

These poly(tartaramide)s are made of flexible polymethylene segments and tartaramide units locked by the acetal ring which visibly protrudes from the backbone. The polymer chain may be then envisaged as composed of an alternating sequence of thread-like hydrophobic and ball-like hydrophilic units.

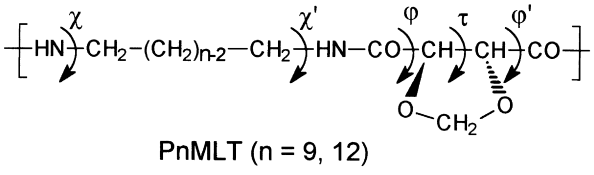

PnMLT (n = 9, 12)

2. Experimental

The polyamides P9MLT and P12MLT investigated in this work were prepared by polycondensation in solution of bis(pentachlorophenyl) 2,3-*O*-methylene-L-tartrate with 1,9-nonanediamine and 1,12-dodecanediamine activated as *N*,*N*′-bis(trimethylsilyl) derivatives. A detailed account of this synthesis has been published elsewhere [13] and a survey of the polymer characteristics more relevant to the present work are given in Table 1. (4*R*,5*R*)-4,5-bis(dodecylcarbamoyl)-1,3-dioxolane used as model compound in spectroscopy studies was prepared by reaction of the above mentioned pentachlorophenyl ester with a large excess of 1,12-dodecanediamine and then purified and characterized by usual methods.

Polymer films were prepared by casting either in formic acid or in chloroform and fibers were obtained by stretching from concentrated solutions of the polymer in such solvents. Optical microscopy was performed with a Nikon Labophot polarizing microscope fitted with a hot stage Mettler FP-80 and a Nikon FX-35DX camera. Melting, crystallization and annealing experiments were carried out on a Perkin–Elmer DSC-4 instrument using 3–5 mg of polymer samples. Thermograms were recorded at heating or cooling rates of ±20°C min^{-1} and they were calibrated with indium. Densities were determined by the flotation technique using mixtures of water and a 25% (w/w) sodium bromide aqueous solution. X-ray diffraction patterns were registered in an evacuated flat-film Warhus camera with Ni-filtered Cu-Kα radiation of wavelength 1.54 Å. Calibration was internally made with molybdenum sulfide ($d_{002} = 6.147$ Å). Single crystals were grown by isothermal crystallization from very dilute solutions (less than 0.1%) of the polymer in 2-octanol or ethyleneglycol. Crystals were recovered by centrifugation and then repeatedly washed with *n*-butanol. For electron microscopy observations in the bright field mode, crystals were deposited on carbon-coated grids and shadowed with Pt–carbon at an angle of about 15°. Electron diffraction diagrams were recorded in the selected area mode and internally calibrated with gold ($d_{111} = 2.35$ Å). A Philips EM-301 electron microscope operating at 80 and 100 kV for bright field and electron diffraction modes, respectively, was used in this work.

Infrared spectra from both, solutions and solid films, were registered on a Perkin–Elmer FT-IR 2000 instrument equipped with a variable temperature cell Specac P/N 21525. NMR experiments were performed on an AMX-300 Bruker spectrometer provided with a CP-MAS solid state accessory. Solution spectra were recorded in chloroform using TMS as reference. Solid state CP-MAS ^{13}C spectra were recorded from 100–200 mg weight samples spun at 3.9–4.1 kHz in a cylindrical ceramic rotor. These spectra were acquired with contact and repetition times of 1.2 ms and 5 s, respectively. Between 256 and 1024 ransients were accumulated using a spectral width of 31.2 kHz. Chemical shifts were externally calibrated against the higher field peak of adamantane which is 29.5 ppm relative to TMS.

To analyze the molecular conformation of model compounds, semi-empirical quantum mechanical calculations were performed with the MOPAC 6.0 package [22] following the same methodology used in previous works [18]. Calculating programs were run on an IBM SP2 at the Centre de Supercomputació de Catalunya (CESCA) and on a Silicon-Graphics station RI-4000 at our laboratory.

3. Results and discussion

3.1. Poly(dodecamethylene 2,3-di-O-methylene-L-tartaramide) (P12MLT)

3.1.1. Optical microscopy and DSC measurements

P12MLT films prepared by different methods were

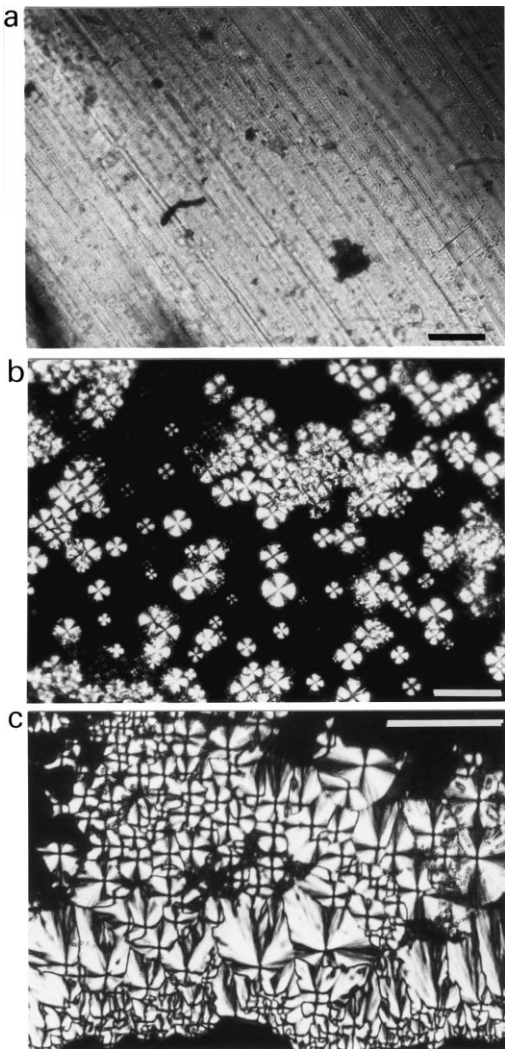

Fig. 1. Polarizing optical micrographs of P12MLT. (a) Birefringent film prepared by hot-pressing at 150°C. (b) Spherulites crystallized at 115°C from the film shown in (a). (c) Spherulitic film prepared by casting from formic acid at low evaporation rate.

examined under a polarizing optical microscope. Films generated at high solidification rates either from solution or from the melt appeared uniformly dark but displayed strong birefringence upon slightly shearing. Conversely, striking colorful films were obtained by hot-pressing above 150°C (Fig. 1a). Such optical effects strongly suggest the existence of a mesophase-like structure. When hot-pressed films were heated at 100°C all signs of birefringence disappeared and further heating at 110–115°C induced spherulitic crystallization (Fig. 1b). Spherulites vanished when temperature reached 130°C, which is taken as the melting temperature of the polymer. On the other hand, highly crystalline films composed of impinging spherulites were produced by casting in formic acid or chloroform at low evaporation rates (Fig. 1c).

The calorimetric behavior displayed by P12MLT is illustrated in Fig. 2 where the DSC traces and powder X-ray patterns of two samples with different histories are compared. Fast-formed films produced a thermogram containing two endotherm peaks with maxima at 105 and 120°C. Conversely, samples obtained either by casting at low evaporation rates or by crystallization from the melt at 115°C for a few hours produced thermograms consisting of a single endotherm at 130°C. The diffraction pattern recorded from the former contains two discrete rings in addition to an outer diffuse halo indicative of a partially ordered phase. On the contrary, a highly crystalline diagram with more than ten sharp rings was obtained from slowly crystallized samples. Annealing at 115°C of the poorly crystallized polymer not only removed the low temperature peak but also caused the displacement of the second peak up to near 130°C. Well-defined diffraction patterns were recorded from the annealed sample. These results indicate that the 120°C peak observed in the fast-formed film traces arises from crystallites generated in a fusion–crystallization process taking place in the 100–120°C range. This is in full agreement with observations made under the polarizing microscope.

Two phases are therefore identified for P12MLT on the basis of the observations accounted above: a highly crystalline phase that is formed under quiescent crystallization conditions and a partially ordered phase that is adopted when the transient of the polymer from liquid to solid proceeds at high rates. Such largely kinetics-dependent behavior is in agreement with the semi-flexible nature of the polymer chain.

3.1.2. X-ray diffraction and electron microscopy

X-ray diffraction patterns of P12MLT oriented by stretching from chloroform and from formic acid solutions are shown in Fig. 3. In the former case, the pattern consists of a series of discrete reflections on the meridian associated to a basic spacing of 20 Å and a diffuse arced spot with a spacing around 4.5 Å equatorially oriented (Fig. 3a). This is the pattern that should be expected from a uniaxially oriented structure lacking lateral order. On the other side, the fiber obtained in formic acid produced a pattern displaying reasonable sharp reflections on both the meridian and the equator indicating that the polymer has crystallized in a three-dimensional lattice (Fig. 3b). Annealing of the poorly ordered film coming from chloroform at temperatures near to the melting point of the polymer was found to induce the lateral crystallization of the chains, in agreement with previous DSC observations.

Comparison of X-ray patterns shown in Figs. 2 and 3 reveals that isotropic and uniaxially oriented samples of P12MLT exhibit similar degree of order provided that the polymer is solidified at similar rates or subjected to the same thermal treatment. Diffraction data provided by partially disordered patterns are consistent with a smectic liquid crystal phase with the strata separated by a spacing of 20 Å. On the other hand, crystalline patterns may be satisfactorily indexed on the basis of a crystal lattice of orthorhombic geometry and a subcell of parameters $a_0 = 7.75$ Å,

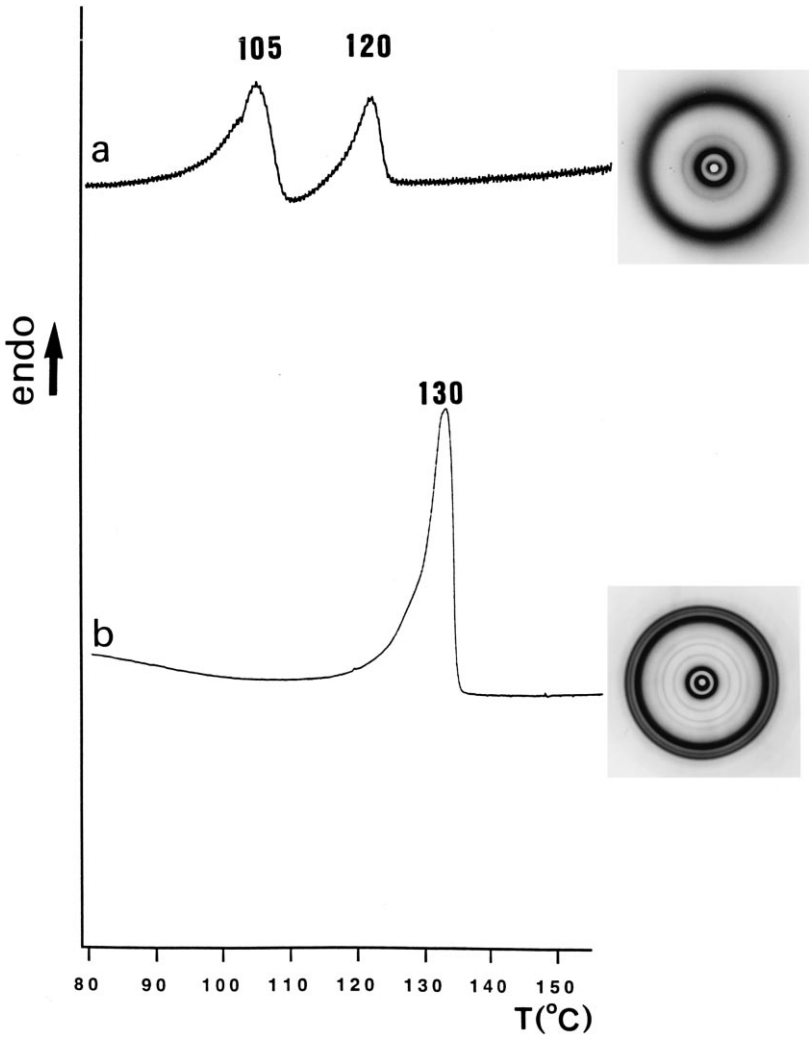

Fig. 2. Heating DSC traces and corresponding powder X-ray diagrams of P12MLTsamples. (a) Poorly crystallized polymer. (b) Film prepared by slow evaporation of a formic acid solution.

$b_0 = 5.85$ Å and $c_0 = 20.0$ Å containing two chemical residues (Table 2). It should be noted that the structural chain repeat comprises two chemical residues indicating that c_0 must be probably doubled. The calculated density for this structure is 1.20 g ml^{-1}, in excellent agreement with the experimentally found value which is 1.19 g ml^{-1}. It should be noted that the same axial repeat of 20 Å is shared by the two phases of P12MLT and that this distance is ~2.25 Å shorter than the length calculated for the chemical repeating unit of the polymer in fully extended conformation.

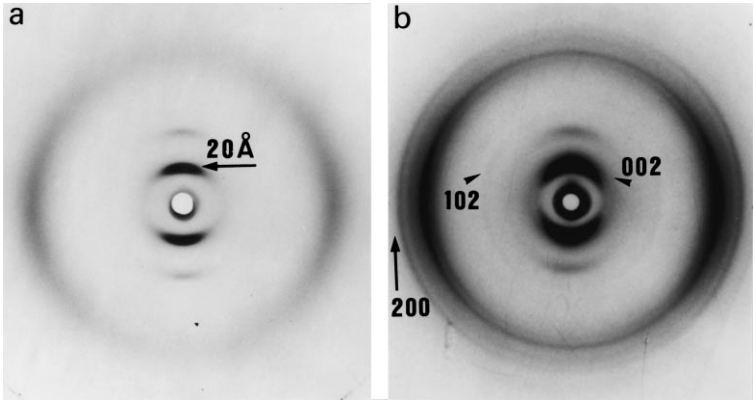

Fig. 3. X-ray diagrams of oriented films of P12MLT. (a) Film prepared by stretching from chloroform. (b) Film prepared by stretching in formic acid.

Table 2
Observed and calculated spacings (Å) for P12MLT

	Observed[a]			Calculated[b]	*hkl*[b]
	Fiber[c]	Crystal mat[d]	Single crystal[e]		
Meridional					
		120 (m)		120.0	L_0 (lamellar height)
		40 (w)		40.0	3rd order
	20.0 (vs)	20.0 (vs)		20.0	6th order and 001
		15.0 (m)		15.0	8th order
		12.5 (w)		12.0	10th order
	10.0 (m)	10.0 (s)		10.0	12th order and 002
		8.5 (vw)		8.6	14th order
		7.5 (vw)		7.5	16th order
	6.8 (w)	6.8 (m)		6.7	18th order and 003
Equatorial					
		5.80 (w)	5.80 (w)	5.85	010
	4.67 (s)	4.65 (vs)	4.60 (vs)	4.67	110
	3.86 (s)	3.85 (vs)	3.88 (vs)	3.88	200
			2.90 (w)	2.92	020
			1.94 (m)	1.94	400
			1.30 (vw)	1.29	600
Off-meridional					
	7.24 (m)	7.30 (m)		7.23	101
	6.25 (w)	6.10 (m)		6.12	102
		5.05 (w)		5.05, 5.05	012, 103
	4.47 (vs)	4.40 (vs)	4.50 (s)	4.55, 4.41	111
	4.15 (m)	4.10 (s)		4.23, 4.20	112, 104
		3.85 (s)		3.82, 3.80	113, 014
	3.60 (w)	3.60 (m)		3.55	105
	3.30 (w)	3.30 (w)		3.30	015
	3.08 (w)	3.10 (m)		3.06, 3.04	106, 115

[a] Intensities visually estimated and denoted as: vs = very strong, s = strong, m = medium, w = weak, vw = very weak.
[b] Spacings calculated and indexed on the basis of a unit cell with $a_0 = 7.75$ Å, $b_0 = 5.85$ Å and $c_0 = 20.0$ Å, $\alpha = \beta = \gamma = 90°$.
[c] Fiber obtained by stretching from formic acid.
[d] Mat of single crystals grown at 83.5°C in 2-octanol.
[e] Measured on single crystal electron diffraction patterns.

Isothermal crystallization of P12MLT in 2-octanol at 83.5°C rendered the type of lamellar crystals shown in Fig. 4. They appear to be very uniform in both shape and size with lateral dimensions of about 4 μm × 2 μm and a thickness of about 120 Å as estimated from electron micrographs of Pt–carbon shadowed specimens. Although the lenticular habit displayed by these crystals is reminiscent of lozenges, their serrated edges and rounded contours make difficult a reliable measurement of their morphological parameters. Crystallization in ethyleneglycol at room temperature provided crystals with abundant overgrowths but displaying sharper outlined contours and revealing a genuine diamond habit with an acute angle close to 70° (inset Fig. 4b).

Electron diffraction diagrams obtained from the crystals grown in 2-octanol consist of a rectangular array of reflections with $a_0 = 7.86$ Å and $b_0 = 5.80$ Å (inset Fig. 4a). The pattern may be straightforwardly interpreted as arising from the projection down the *c*-axis of the crystal lattice defined above. The orientation of the pattern relative to the crystal indicates that the lattice must be aligned with the *a*-axis parallel to the long dimension of the lamella. Systematic absences for *h*00 reflections with $h = 2n + 1$ are detected along the reciprocal *a*-axis in agreement with the existence in the crystal of a 2_1 axis parallel to *a*. All the independent *d*-spacings observed in the original photographic films together with their corresponding indexes are listed in Table 2. It should be noticed that *hk*0 reflections with $h = k$ appear split revealing that more than one reciprocal plane are being intersected by the Ewald sphere. This does make sense since we are dealing with thin platelets crystals composed of a unit cell with a large c_0-parameter.

3.1.3. Infrared spectroscopy

X-ray studies carried out on crystallized *N*-alkyl L-gluconamides have shown that these compounds tend to crystallize in a *skew* conformation stabilized by both intermolecular O–H···O=C and intramolecular N–H···O hydrogen bonds, the latter being of a bifurcated nature with both carbonyl and hydroxyl groups acting as hydrogen-accepting groups [23]. The presence of the 1,3-dioxolane ring in PnMLT makes advisable to investigate in detail

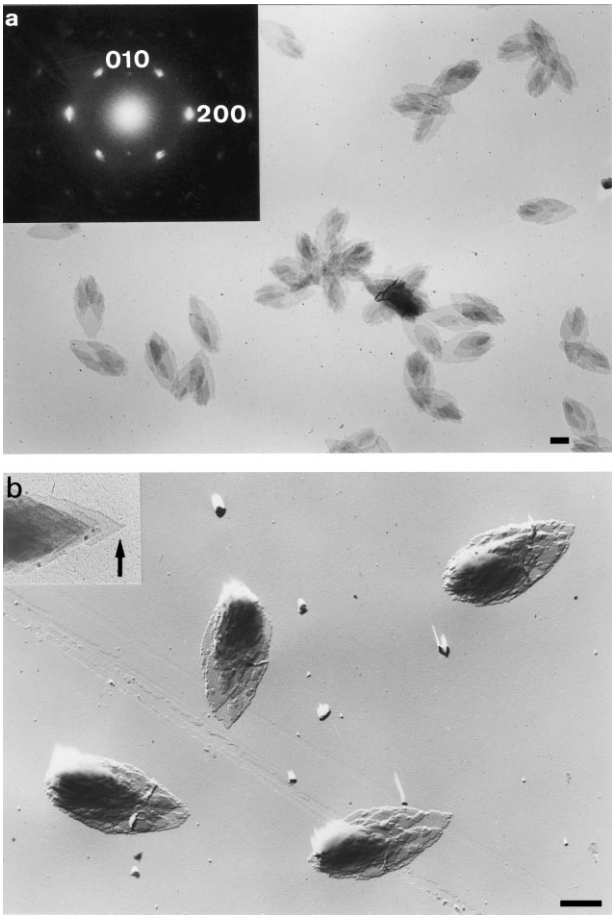

Fig. 4. Lamellar crystals of P12MLT grown in 2-octanol at 83.5°C. (a) Low magnification micrograph illustrating the size and shape homogeneity of the crystals. Inset: electron diffraction patterns arising from one of these crystals oriented as arrowed. (b) Magnified view of selected crystals revealing morphological details. The inset shows the tip of a diamond-shaped crystal grown in ethyleneglycol at room temperature. The bar represents 1 μm.

the nature of hydrogen bonding in these systems. At this aim P12MLT and the model compound (4*R*,5*R*)-4,5-bis(dodecylcarbamoyl)-1,3-dioxolane were examined by infrared spectroscopy, both in solution and in solid films. The 3500–3150 and 1750–1600 cm^{-1} regions containing the absorption bands arising from NH and CO stretching vibration modes respectively were used to study the hydrogen bond interactions as a function of temperature. Results from this study are illustrated in Fig. 5 and the characteristic NH and CO absorption frequencies observed for different P12MTA samples and the model compound are compared in Table 3.

The spectra of both the polymer and the model compound in dilute chloroform solution displayed intense peaks around 3420–3430 and 1670 cm^{-1} attributable respectively to the stretching of NH and CO in the free state. Sharp peaks at 3300 and 1645 cm^{-1} arising from associated amide groups were observed in the spectra recorded from the crystallized model compound. Conversely, the spectrum of P12MLT in the solid state was found to be more complex and highly depending on the history of the sample. Extreme cases are compared in Fig. 5a; films prepared by quenching from the melt or by rapid evaporation of chloroform solutions give a strong broad absorption centered around 3320 cm^{-1} and a single peak at 1660 cm^{-1}. On the contrary, the spectrum from a sediment of single crystals shows main peaks at 3360 and 1670 cm^{-1} with shoulders at 3390 and 1690 cm^{-1}, respectively. Whereas, absorption bands at 3360 and 3320 cm^{-1} can be made to correspond to hydrogen bonded NH located in the crystalline and non-crystalline phases respectively, the origin of the shoulder at 3390 cm^{-1} remains unclear. At any case the fraction of non-bonded amide groups is of minor importance whichever is the degree of ordering attained by the polymer.

Infrared spectroscopy reflected also the effects of thermal treatments on hydrogen bonding in P12MLT. Changes taking place in the spectra of a quenched sample upon heating from room temperature up to 225°C are shown in Fig. 5b. As expected, a continuous shift towards higher frequencies was observed for the 3320 and 1660 cm^{-1} peaks whereas the 3420 cm^{-1} shoulder presumably arising from free NH remained unchanged. The initial spectrum could be fully recovered after cooling. Such behavior is typical of uncrystallized polyamides and it is currently interpreted as due to the weakening of hydrogen bonds caused by temperature [24]. However, the abrupt displacement observed at the surroundings of 100–125°C is unexpected and it should be related to the recrystallization process taking place in P12MLT within this range of temperatures. On the other hand, crystallization taking place upon annealing of a quenched sample of P12MLT at 125°C (Fig. 5c) produces jumps in both NH and the CO stretching frequencies after 5 h of treatment.

We can conclude from these results that hydrogen bonding in the model compound is stronger than in the polymer, and that such interactions become weaker as the degree of order of the polymer increases. The situation is similar to that known to occur in conventional nylons where chains crystallize in fully extended conformation [25]. In the present case, the disturbing effect responsible for the weakening of the hydrogen bonds in the crystal phase is thought to arise from accommodation of the dioxolane ring in the lattice.

3.1.4. NMR spectroscopy

CP-MAS ^{13}C NMR studies carried out on P12MLT and (4*R*,5*R*)-4,5-bis(dodecylcarbamoyl)-1,3-dioxolane provided invaluable information on conformation and packing of the polymer in the solid state. In an earlier work, ^{13}C NMR spectra of the model compound in solution showed satellite signals of cyclic methine protons demonstrative of a puckered conformation with the isoenergetic C_2-*endo* and C_2-*exo* envelope forms in fast interconversion [26]. The ^{13}C NMR spectrum of P12MTA in chloroform solution shows similar features indicating that the dioxolane ring in the polymer must be in the same interconverting folded conformation.

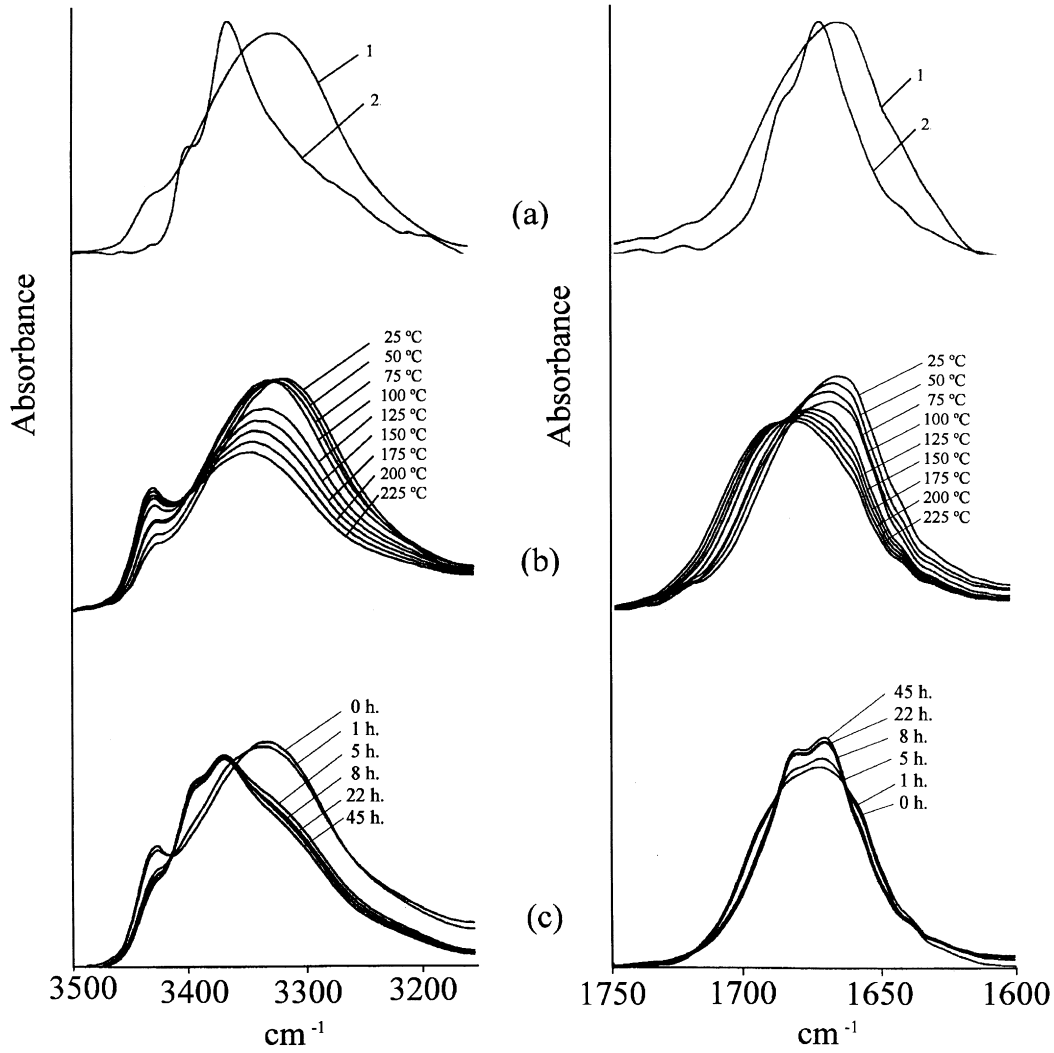

Fig. 5. (a) Compared 3500–3150 cm^{-1} infrared spectra of P12MLT at room temperature 1 = quenched sample; 2 = single crystal sediment. (b) Evolution of the NH and CO bands in a film quenched from the melt and heated from 25 to 225°C at intervals of 25°C. (c) Changes in the spectrum of the quenched film with annealing at 125°C for the indicated periods of time.

The CP-MAS ^{13}C NMR spectrum of a quenched sample of P12MLT shows single peaks for both the methylene and the two magnetically equivalent methyne carbons of the dioxolane ring as well as for the carbonyl carbon (Fig. 6a). Similar features were displayed by the spectrum of this compound in chloroform solution (Table 4). On the contrary, split signals with a separation between peaks of 2–5 ppm were observed for both the methyne and the

Table 3
Infrared NH and CO stretching frequencies (cm^{-1}; frequency values rounded to tenths. Relative intensities of peaks denoted as: s = strong, sh = shoulder, w = weak) for P12MLT and the model compound (4*R*,5*R*)-4,5-bis(dodecylcarbamoyl)-1,3-dioxolane

	NH				CO	
	Free	Associated			Free	Associated
Model compound						
Cl_3CH solution	3420s				1670s	
Crystallized				3300s		1645s
P12MLT						
Cl_3CH solution	3430s			3320w	1690s	1660sh
Single crystals		3390sh	3360s		1690sh	1670s
Quenched	3420w			3320s		1660s
Annealed	3420w	3390sh	3360s	3320sh	1690sh	1670s

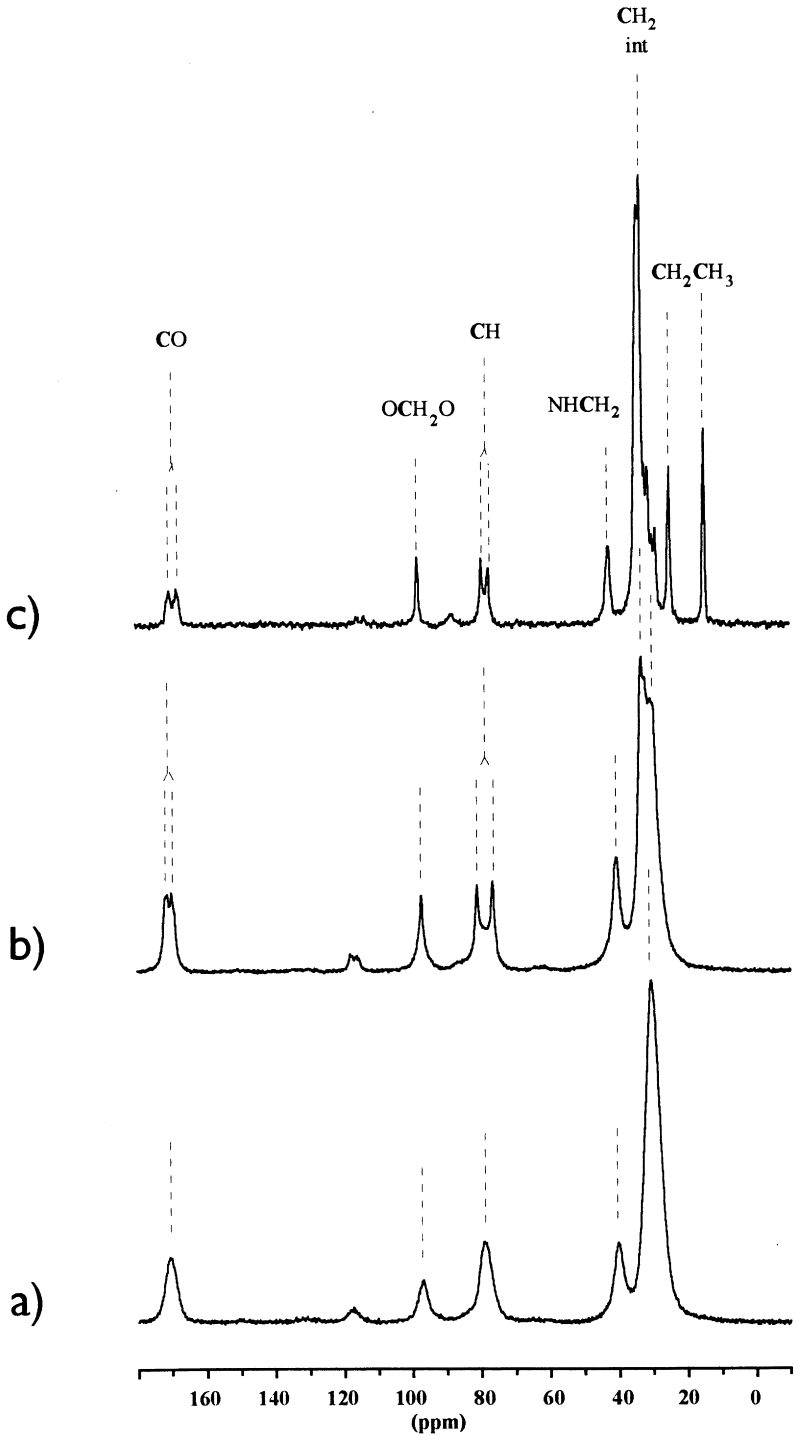

Fig. 6. CP-MAS ^{13}C NMR spectra of P12MLT. (a) Quenched sample. (b) Film casted in formic acid. (c) Model compound (4*R*,5*R*)-4,5-bis(dodecylcarbamoyl)-1,3-dioxolane.

carbonyl carbons in the spectrum obtained from crystallized P12MLT (Fig. 6b). The spectrum is similar in this regard to that obtained from the model compound in the crystalline state (Fig. 6c). These observations are consistent with the occurrence of a puckered conformation for the dioxolane ring containing equal populations of the frozen C_2-*exo* and C_2-*endo* forms. Similar conformational effects on chemical shifts of ^{13}C NMR solid state spectra have been reported for certain epoxydic polymers [27]. Furthermore, the fact that peaks observed in the spectrum of the quenched polymer are broad indicates that a wide distribution of conformations between the two limiting envelope forms must be present in such sample.

An inspection of the resonance polymethylene region

Table 4
CP-MAS ^{13}C NMR chemical shifts (ppm) for P12MLT and the model compound (4*R*,5*R*)-4,5-bis(dodecylcarbamoyl)-1,3-dioxolane

	CO		OCH_2O	CH		$NHCH_2$	$(CH_2)_{int}$		$\mathbf{C}H_2CH_3$	$CH_2\mathbf{C}H_3$
Model compound	170.2	168.1	98.0	79.3	77.2	42.6	33.2		24.7	14.7
P12MLT										
Crystallized	171.1	169.9	97.2	80.9	76.4	40.7	33.0	30.6		
Quenched	170.8		97.0	79.2		40.4	30.7			
$CHCl_3$ solution	168.9		96.3	77.5		39.4		29.3		

(30–42 ppm) revealed that the signal arising from interior methylenes (C2–C11) in the crystallized polymer consists of two peaks at 30.5 and 33.0 ppm which correlate with those observed for the model compound and the quenched polymer respectively. The downfield peak arises from methylenes arranged in *trans-gauche* whereas the upfield one is attributed to methylenes crystallized in the all-*trans* conformation. Differences of 2.5–3.0 ppm between the methylene signals have been reported for nylon 12 in the crystallized and the amorphous state [25].

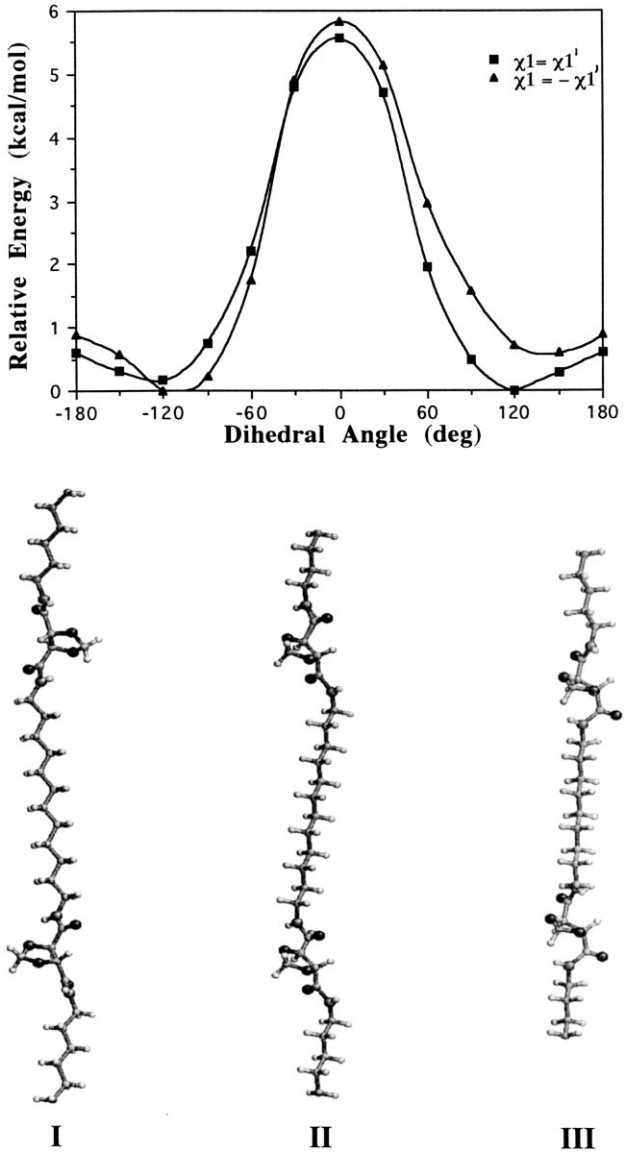

Fig. 7. Conformational profiles of (4*R*,5*R*)-4,5-bis(ethylcarbamoyl)-1,3-dioxolane around the dihedrals χ_1 and χ'_1 and schematic representation of models I and II for the repeating unit of P12MLT and model III for the repeating unit of P9MLT.

3.1.5. Energy calculations

Previous computational work carried out on a set of (4*R*,5*R*)-4,5-bis(alkylcarbamoyl)-1,3-dioxolanes supported by experimental NMR data proved that the two O–C–C=O sequences adopt the same *gauche* conformation with φ and φ' taking values of either +60 or −60° [26]. Assuming that the planar amide groups in the polymer adopt the same orientation respect to the dioxolane ring and that the dodecamethylene chain is in the all-*trans* conformation, energy calculations may be addressed to optimize the torsional angles χ_1 and χ'_1 involved in the movement of the aliphatic segment as a whole. For this purpose, the conformation of the relative simple analogue (4*R*,5*R*)-bis(ethylcarbamoyl)-1,3-dioxolane was analyzed upon rotation around χ_1 and χ'_1 for the cases $\chi_1 = \chi'_1$ and $\chi_1 = -\chi'_1$. Results are compared in Fig. 7 where it becomes apparent that the two profiles are nearly isoenergetic within the whole rotational wheel. Two favored energy regions (+90 to +150° and −90 to −150°) were found in both cases with absolute minima located at +120 and −120°, respectively. The stabilization of these minima relative to the rotamer with $\chi_1 = \chi'_1 = 0$ is about 6 kcal mol^{-1} residue^{-1}. Optimization of the conformation of the whole polymer chain was made for the model molecule (4*R*,5*R*)-bis(hexylcarbamoyl)-1,3-dioxolane. For this, minimum values found for the ethyl derivative were combined and the same constraints considered in the previous stage were imposed. Results indicated that the two models having $\varphi = \varphi' = -60°$ and $\chi_1 = \chi'_1 = -120°$ (model I) and $\chi_1 = -\chi'_1 = +120°$ (model II) are almost isoenergetic and equally probable. These models are depicted in Fig. 7. Model I is a 2_1 helix whereas identity is the only symmetry element found in model II. Both models appear to be compatible with the crystal lattice defined above. Further modeling work is needed in order to specify what would be the favored conformation.

3.1.6. Phases structures

The structures of the two phases observed for P12MLT

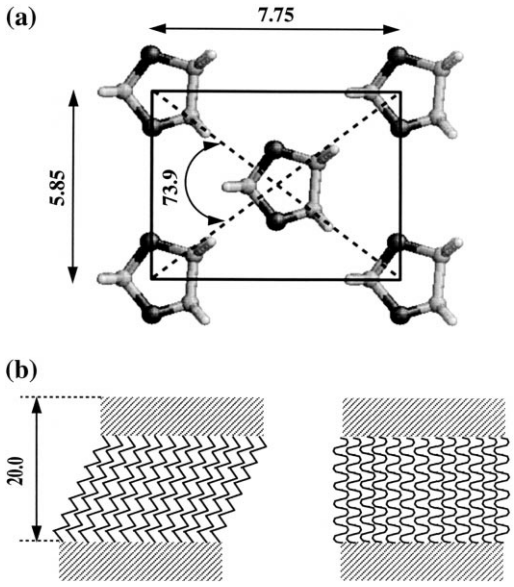

Fig. 8. (a) Unit cell projection down the *c*-axis of the crystal phase of P12MLT. (b) Schematic representation of the on-edged viewed structure of PnMLT in the crystal phase (left) and in the smectic liquid crystal-like phase (right).

are very similar as far as the axial repeat of the structure is concerned. This means that chains are arranged along the *c*-axis in a similar way in both cases. Differences between the two phases arise therefore from differences in the conformation of the polymer chain and in the degree of order achieved in the lateral packing of the chains (Fig. 8).

The partially ordered phase is envisaged as a stratified structure with chains hexagonally packed with statistical axial orientation. Hydrogen bonds between neighboring chains would be set at random in three directions fixing an average interchain distance of about 5 Å. The chains are in axial register so that tartaric units are arranged in planes normal to the axis and separated by 20 Å. The polymethylene segment runs parallel to the axis in a conformation that slightly deviates from all-*trans* in order to be accommodated within the observed axial repeat. The result is a structure lacking three-dimensional order that allows a rather comfortable formation of intermolecular hydrogen bonds compatible with the presence of the protruding dioxolane rings. This structure is thought to be reminiscent of the smectic mesophase that presumably is formed in solution at high polymer concentrations.

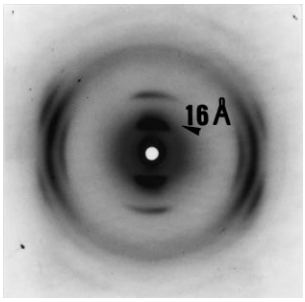

Fig. 9. X-ray diffraction pattern from a fiber of P9MLT obtained by stretching from chloroform and annealed at 80°C.

In the crystalline phase the axial repeat is again 20 Å but polymethylene segments are in all-*trans* conformation and tilted about 15° with respect to the azimuth of the crystal. Dioxolane rings are lying in planes normal to *c*-axis and placed at the kinks of the chains. By this means, hydrogen bonds may be formed between neighboring chains aligned along directions 110 and −110 of the crystal and separated by 4.85 Å. It is noteworthy that such directions are at an angle of 74°, in good agreement with the value measured for the acute angle of the lozenge lamellar crystals. Preliminary modeling work revealed that although hydrogen bonded chains are at the expected distances, the geometry of the hydrogen bond is significantly deviated from standard values. This entails a destabilization of the N–H···C=O interactions in agreement with the relatively high infrared NH and CO frequencies observed in the crystalline phase.

3.2. Poly(nonamethylene 2,3-di-O-methylene-L-tartaramide) (P9MLT)

A parallel study was carried out on the homologous P9MLT in order to evaluate the influence of the polymethylene chain length on the crystal structure of these dioxolane-containing poly(tartaramide)s. As before, films obtained by casting from chloroform produced X-ray diagrams consisting of both discrete and diffuse scattering indicative of a partially ordered structure. However such films were unable to develop spherulitic texture upon annealing. DSC curves of such samples displayed a single endotherm at about 90°C and no crystallization from the melt was observed at any cooling rate. We interpret the DSC peak as due to the melting of a smectic-like phase of similar characteristics to that described for P12MLT. The fact that no crystallization takes place is indicative that chain mobility in P9MLT is even more hindered than in P12MLT. This is according to the higher concentration of tartaric units present in this polymer.

Results with fibers were also similar to those obtained with P12MLT. X-ray diffraction patterns from samples stretched either from the melt or from concentrated solutions display poorly lateral crystallization of the chains. When such fibers were subjected to annealing they yielded diagrams containing sharps reflections characteristic of a three-dimensional ordered structure (Fig. 9). Both crystalline and non-crystalline patterns display an intense meridional reflection with a spacing of about 15 Å corresponding to the axial repeat of the structure. In this case the shortening respect to the fully extended conformation is about 3.75 Å indicating that the polymethylene chains are here even more tilted than in the case of P12MLT. An orthogonal lattice with parameters $a_0 = 4.71$ Å, $b_0 = 12.32$ Å, $c_0 = 16.00$ Å, $\alpha = \beta = \gamma = 90°$ containing two chains can be tentatively proposed for the crystal structure

in analogy to the structure given for P12MLT. The density calculated for such structure is 1.10 g ml^{-1} in excellent concordance with the observed value which was estimated to be 1.08 g ml^{-1}. Optimization of the conformation by energy calculations gave model III with $\varphi = -\varphi' = -60°$ and $\chi_1 = -\chi'_1 = -120°$ as the most favored arrangement for the crystallized P9MLT chain (Fig. 7).

4. Concluding remarks

Two crystalline phases differing in the degree of ordering are adopted by polyamides P12MLT and P9MLT depending on crystallization conditions. At high crystallization rates, a smectic-like phase with defective chain lateral order is developed whilst at low rates a three-dimensional crystal is formed. The favored conformation of these poly(tartaramide)s entails a *gauche* arrangement for the two O–C–C=O sequences comprised in the tartaric unit which accounts in part for the reduction observed in the length of the structural repeating unit of the two polymers. The dioxolane ring is in a puckered conformation with the isoenergetic C_2-*endo* and C_2-*exo* forms in equal amounts and the polymethylene segment is arranged in all-*trans* conformation. Extensive intermolecular hydrogen-bonding takes place in these polyamides both in the ordered and disordered phases. The stability of such interactions decreases with the degree of ordering because of disturbing effects arising from the presence of the bulky acetal side group.

Crystallization of the “smectic” phase may be induced in the solid state by annealing. The process implies a rearrangement in both the side-by-side packing of the chains and the conformation of the polymethylene segment. In the P12MLT crystal lattice the chains describe a wavy trajectory with the straight polymethylene segment tilted about 16° with respect to the azimuth of the crystal and dioxolane cycles accommodate at the kinks. Preliminary data obtained for P9MLT indicate a similar behavior but chains arranged in the crystal with an even higher inclination.

Acknowledgements

Financial support from the CICYT (Comisión Interministerial de Ciencia y Tecnología) for the scientific grant MAT96-1181-CO3-03 is gratefully acknowledged. The authors are indebted to CESCA for computational facilities.

References

[1] Tadokoro H. Structure of crystalline polymers, New York: Wiley, 1979.
[2] Kohan MI. Nylon plastics, New York: Wiley, 1971.
[3] Aharony SM. *n*-Nylons: their synthesis, structure and properties, New York: Wiley, 1997.
[4] Wunderlich B. Macromolecular physics, 1. New York: Academic Press, 1973.
[5] Selegny E, Merle-Aubry L. In: Selegny E, editor. Optically active polymers, Dordrecht: Reidel, 1979. pp. 15–110.
[6] Coiro VM, de Santis P, Mazarella L, Picozzi L. J Polym Sci: Part A 1965;3:4001.
[7] Schmidt E. Angew Makromol Chem 1970;14:185.
[8] Prieto A, Iribarren JI, Muñoz-Guerra S, Bui C, Sekiguchi H. Crystallization of polymers. In: Dosiere M, editor. NATO ASI Series, Serie C, 405. Dordrecht: Kluwer, 1993. pp. 613–8.
[9] Muñoz-Guerra S, López-Carrasquero F, Fernández-Santín JM, Subirana JA. In: Salamone JC, editor. The polymeric materials encyclopedia, Boca Raton, FL: CRC Press, 1996. pp. 4694–700.
[10] Puiggalí J, Muñoz-Guerra S, Rodríguez-Galán A, Subirana JA. Makromol Chem, Macromol Symp 1988;20/21:167.
[11] Bou JJ, Rodríguez-Galán A, Muñoz-Guerra S. In: Salamone JC, editor. The polymeric materials encyclopedia, Boca Raton, FL: CRC Press, 1996. pp. 561–9.
[12] Bou JJ, Iribarren JI, Rodríguez-Galán A, Muñoz-Guerra S. In: Vert M, editor. Biodegradable polymers and plastics, Cambridge, UK: Royal Society of Chemistry, 1992. pp. 271–4.
[13] Rodríguez-Galán A, Bou JJ, Muñoz-Guerra S. J Polym Sci: Polym Chem Ed 1992;30:713.
[14] Bou JJ, Rodríguez-Galán A, Muñoz-Guerra S. Macromolecules 1993;26:5664.
[15] Bou JJ, Muñoz-Guerra S. Polymer 1984;36:181.
[16] Bou JJ, Iribarren JI, Muñoz-Guerra S. Macromolecules 1994;27:5263.
[17] Bou JJ, Iribarren JI, Martínez de Ilarduya A, Muñoz-Guerra S. J Polym Sci: Polym Chem Ed 1999;39:983.
[18] Iribarren JI, Alemán C, Bou JJ, Muñoz-Guerra S. Macromolecules 1996;29:4397.
[19] Chen L, Kiely DE. Polym Prepr Am Chem Soc, Div Polym Chem 1993;34:550.
[20] Chen L, Kiely DE. J Org Chem 1996;61:5847.
[21] Bandrup J, Immergut H. Polymer handbook, VII. New York: Wiley, 1989 p. 25.
[22] Stewart JJP. MOPAC 93 Rev 2, Fujitsu Ltd, 1993.
[23] Müller-Fahrnow A, Hilgenfeld R, Hesse H, Saenger W, Pfannemüller B. Carbohydr Res 1988;176:175.
[24] Skrovanek DJ, Howe SE, Painter PC, Coleman MM. Macromolecules 1985;18:1676.
[25] Mathias LC, Johnson CG. Macromolecules 1991;24:6114.
[26] Alemán C, Martínez de Ilarduya A, Giralt E, Muñoz-Guerra S. Tetrahedron 1996;52:8275.
[27] Garroway AN, Ritchey WM, Moniz WB. Macromolecules 1982;15:1051.